16th Australasian Fluid Mechanics Conference
Crown Plaza, Gold Coast, Australia
2-7 December 2007

Influence of Fuel Type on Turbulent Nonpremixed Jet Flames Under MILD Combustion Conditions

P. R. Medwell, P. A. M. Kalt and B. B. Dally

School of Mechanical Engineering
The University of Adelaide, South Australia, 5005 AUSTRALIA

Abstract

This paper reports on the systematic variation of fuel type for turbulent nonpremixed flames issuing into a heated and diluted coflow. The coflow oxidant stream achieved using the jet in hot coflow (JHC) burner emulates MILD (Moderate or Intense Low oxygen Dilution) combustion conditions. Combined laser diagnostic imaging simultaneously reveals the in-situ spatial distribution of the hydroxyl radical (OH), formaldehyde (H_2CO) and temperature. In this work, three different fuels are considered, viz., natural gas, ethylene, and LPG (each diluted with hydrogen). The influence of the fuel chemistry on the flame behaviour and reaction zone structure is examined. It is observed that under MILD combustion conditions there does not seem to be a significant effect of the fuel type on the structure of the reaction zone. The fluidic structure of the turbulent jet appears to control the flame more so than the chemistry in the MILD combustion conditions of the JHC burner.

Introduction

Heat and exhaust gas recirculation in combustors is an innovative approach to create a distributed reaction zone, reduce pollutant emissions and increase the net radiation flux, and with it thermal efficiency. It is now well established that a mixture of reactants diluted with combustion products, at a temperature above auto-ignition, can achieve the desired outcome of reduced pollutant emissions and enhanced thermal efficiency. The application of these principles to practical systems has taken different routes and different names used to describe the process. Some relied on a descriptive form of the resulting combustion process, i.e. Flameless Oxidation (FLOX®) [12] and others described the features of the reactants streams, i.e. High Temperature Air Combustion. The term used in this paper is Moderate or Intense Low oxygen Dilution (MILD) combustion [2].

The MILD combustion technology has been successfully applied in several industries [13], and has the potential for introduction into numerous other applications [2]. To date however, implementation has been impeded by a lack of fundamental understanding of the establishment and detailed structure of this combustion regime. Few fundamental studies have been performed to look at the detailed structure of this regime (e.g. [1, 2, 4, 7, 8]).

The current project is part of a concerted effort to examine the structure of the reaction zone by using laser diagnostic techniques to instantaneously and simultaneously image the distribution and concentration of the two key flame intermediates hydroxyl radical (OH) and formaldehyde (H_2CO). Under conventional combustion conditions OH has long been used as a flame front marker, whereas under MILD conditions Dally [3] has shown that OH concentrations are comparatively minor, and H_2CO appears to dominate. Moreover, the product of $[OH]$ and $[H_2CO]$ has been suggested as an indicator of the formyl (HCO) radical, which is closely related to the heat release rate [9].

The depleted O_2 oxidant at elevated temperatures, necessary for MILD combustion, is typically realised by the recirculation of hot exhaust gases. Recirculation may be achieved either internally or externally with regard to the combustor. The complex interactions within such a system make it unsuitable for a fundamental study of the reaction zone. Instead, an experimental burner is used to emulate MILD combustion under controlled conditions, enabling a range of combustion parameters to be varied independently, and decoupling the flow from the chemical kinetics.

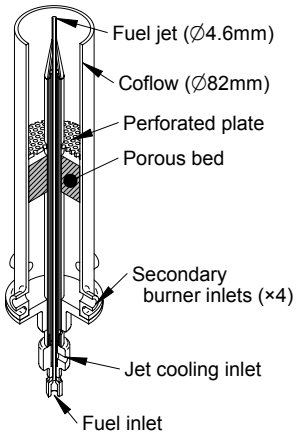

Figure 1: Cross-sectional view of jet in hot coflow (JHC) burner.

In this paper the influence of combustion chemistry on the flame behaviour and reaction zone structure is examined by systematically increasing the fuel complexity under MILD combustion conditions. Three different fuels are considered, namely; natural gas, ethylene, and LPG (each diluted with hydrogen). The difference in the chemical path for these fuel mixtures provides a way of assessing the sensitivity of the MILD combustion regime to fuel type (for gaseous hydrocarbon fuels). By maintaining all other conditions constant except for the fuel type, any differences between the flame structure can be attributed to the chemical kinetics of the fuel.

For each fuel type in the jet, differences in the fluid properties necessitates a change in the velocity to hold the Reynolds number constant (at Re_{jet}=10,000) in order to maintain similar turbulence levels. The primary fuel is diluted with hydrogen (H_2) in an equal volumetric ratio to reduce the levels of soot and to improve flame stability. Addition of H_2 also has implications for the potential use of hydrogen as a supplemental fuel additive.

Experimental Details

The MILD combustion burner used in this study is the jet in hot coflow (JHC) burner used previously [7, 8], and shown in Figure 1. It consists of a central insulated fuel jet (⌀4.6mm) within an annular coflow (⌀82mm) of hot exhaust products from a sec-

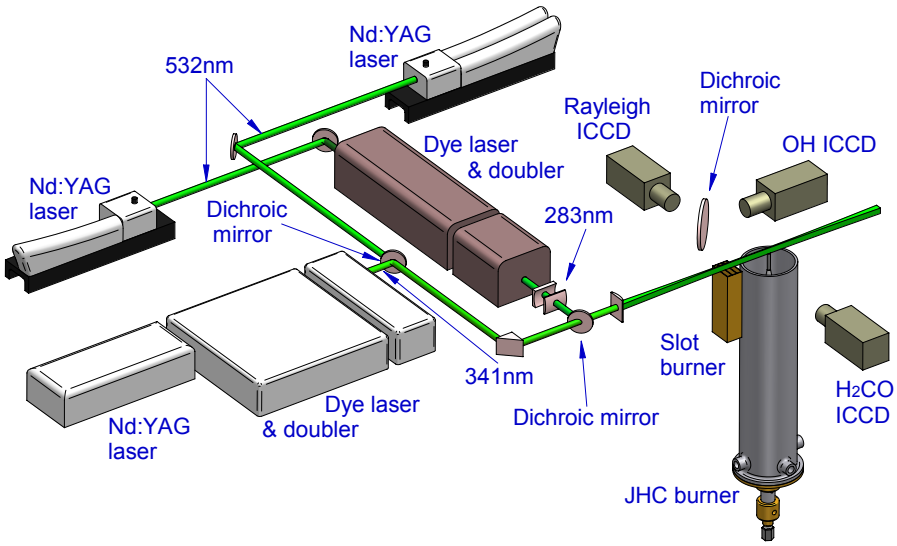

Figure 2: Schematic of experimental layout.

ondary burner mounted upstream of the jet exit plane. The fuel jet is more than 100 diameters in length to ensure fully developed pipe flow. The outer annulus is insulated with a fibrous blanket to minimise heat losses to the surrounds. The influences of the coflow remain ∼100mm downstream of the jet exit plane, beyond this the surrounding air begins to mix with the jet and coflow. The surrounding air entrainment facilitates the additional study of these effects on the reaction zone [8].

The O_2 level of the coflow is controlled by the constant flowrate secondary porous burner. The ratio of the coflow air/nitrogen was varied to give coflow O_2 levels of 3% or 9% (volumetric), while the temperature and exit velocity was kept constant at 1100K and 2.3m/s. Based on the annulus diameter the coflow Reynolds number is ∼1400.

Various hydrocarbon fuels are used in the jet; natural gas (NG), ethylene (C_2H_4) and LPG. Each primary fuel is diluted with hydrogen (H_2) in an equal volumetric ratio to reduce the levels of soot and to improve flame stability. Without H_2 in the fuel stream the flames were seen to blowoff. Jet Reynolds number (based on jet diameter and mean exit velocity) for this paper is fixed at 10,000 for the three different fuel compositions.

Laser induced fluorescence (LIF) is used to image OH and H_2CO, and temperature is inferred from Rayleigh scattering measurements. Each species is probed with a separate laser system. Excitation of OH is at 283.222nm $(A-X\ (1,0)\ Q_1(7))$, and H_2CO via $A-X\ \left(2_0^1 4_0^1\right)\ ^pQ_{21}(5)$ at 340.836nm. The two LIF laser beams were produced from the frequency doubled output of dye lasers (Nd:YAG pumped at 532nm). The output power of the dye lasers was ∼2mJ/pulse for OH and ∼10mJ/pulse for H_2CO, with measured linewidths of 0.5cm^{-1} and 0.26cm^{-1} for OH and H_2CO, respectively. The source for the Rayleigh scatter was a ∼160mJ/pulse 532nm beam from a Nd:YAG laser. Detailed description of the LIF excitation schemes has previously been presented [8].

The experimental layout is shown in Figure 2. The three laser wavelengths are formed into overlapping co-planar laser sheets. The laser sheets pass through a laminar slot burner (for reference purposes) in the same field of view as the JHC burner. The laser pulses are fired sequentially to reduce interferences on the other systems, with the entire sequence occurring in 300ns to ensure the flow field is frozen in time. Each species is detected normal to the laser sheet with a gated intensified CCD (ICCD) camera. To accommodate three separate cameras, a dichroic mirror is used between the OH and Rayleigh cameras. The dichroic reflectance is greater than 80% in the range 270–340nm, therefore acting as a broadband filter for the OH camera. The H_2CO and Rayleigh cameras were each fitted with long wave pass optical filters, GG-385 and GG-495 respectively. To minimise elastic scatter from particulate matter, gases were filtered and measurement locations chosen which were free of visible soot. The Rayleigh and H_2CO cameras were both used with $f_{\#}1.2$ lenses, and OH with a $f_{\#}4.5$ lens. The in-plane resolution of all three ICCD cameras is 160µm, after spatial matching. The light sheet thicknesses are estimated to be slightly larger than this, but of a similar order based on burns from photosensitive paper. The laser sheet heights were all ∼12mm, of which the central 8mm portion is presented herein. Further description of the experimental layout has been outlined in previous publications by the authors, e.g. [8].

The images from the three ICCDs are spatially matched to ensure that each pixel corresponds to the same point in the flame. Each image is corrected for dark-charge and detector attenuation and also for laser power and profile variations shot-to-shot based on the signal from the laminar slot burner.

The temperature and composition change quite considerably both throughout the measurement volume and with different flame conditions. To account for these effects, consideration is given to the ground-state Boltzmann population distribution and collisional quenching effects. The specific correction procedures for the LIF and Rayleigh data are described in-depth in a previous publication by the authors [8]. Error analysis and a discussion of issues regarding measurement interference are also included in other publications [7, 8].

Results

Visual Observations

Figure 3 shows photographs of the flames presented in this paper. Apparent from Figure 3 is that the natural gas flames show significantly less soot than the ethylene and LPG flames. While soot is seen at both coflow O_2 levels for the ethylene and LPG flames, at the 3% O_2 level soot does not appear until around ∼200mm downstream, whereas for the 9% O_2 case soot appears

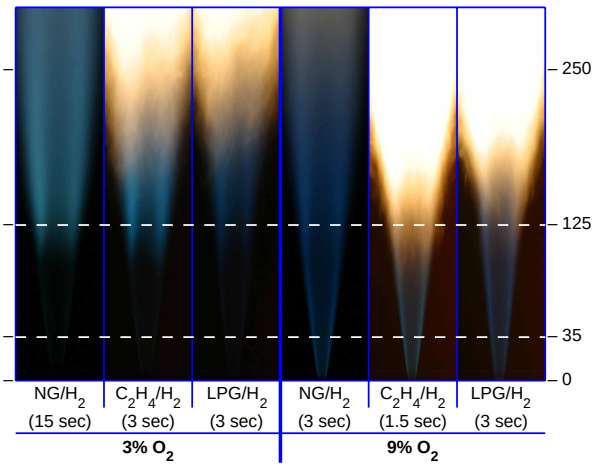

Figure 3: Photographs of natural gas (NG), ethylene (C_2H_4) & LPG flames, each diluted with hydrogen (1:1 vol/vol) at two coflow O_2 levels. Jet Reynolds number of 10,000. Note the different exposure times (all other camera parameters held constant). Horizontal lines indicate measurement locations (35mm & 125mm downstream of jet exit plane). Photograph height: 300mm.

much closer to the jet exit (∼100mm). For either fuel type, at the higher (9%) O_2 level, close to the jet exit the flame luminosity is significantly greater as compared to the lower (3%) O_2 case. The low luminosity of the 3% O_2 flames almost makes them appear invisible for the first ∼100mm. While not clearly apparent from the photographs, a faint reaction is indeed apparent in this region. Further downstream, once the effects of the coflow are diminished by the entrainment of surrounding air, soot does begin to appear for either coflow O_2 level. The presence of soot around the 125mm downstream location in the 9% O_2 flames could potentially interfere with laser diagnostic measurements, and so data is collected at this location for the 3% O_2 flames only.

Typical Features

Figure 4 presents typical image triplets of OH, H_2CO and temperature for each flame condition (three fuel types, each at two coflow O_2 levels). The measurements are centred at 35mm downstream of the jet exit plane. The corresponding size of each image is 8mm in height and 35mm wide. The jet centreline is marked by the vertical dashed line. These images are for a jet Reynolds number of 10,000 and are typical of other Reynolds number flames as well. Despite the flow being nominally turbulent, the majority of the images show no sign of large-scale turbulent structure.

In each of the images presented in Figure 4 the OH appears as an unconvoluted layer which is quite uniform in intensity along the length of the sheet. For each fuel type, the OH concentration is considerably less at 3% O_2 as compared to the 9% O_2 case. The suppression of OH with a reduction in O_2 level is consistent with previous work (e.g. [8, 11]) and is directly related to the reduced temperature of the reaction zone. At either O_2 level the OH concentration does not significantly vary with the fuel type.

The temperature in the coflow is seen to be uniform. With the 9% O_2 coflow the temperature is seen to increase in the region corresponding to OH. For all of the 3% O_2 cases there is no obvious sign of a temperature increase across the reaction zone, although a reaction is clearly taking place as identified by the presence of OH. Similar observations regarding the

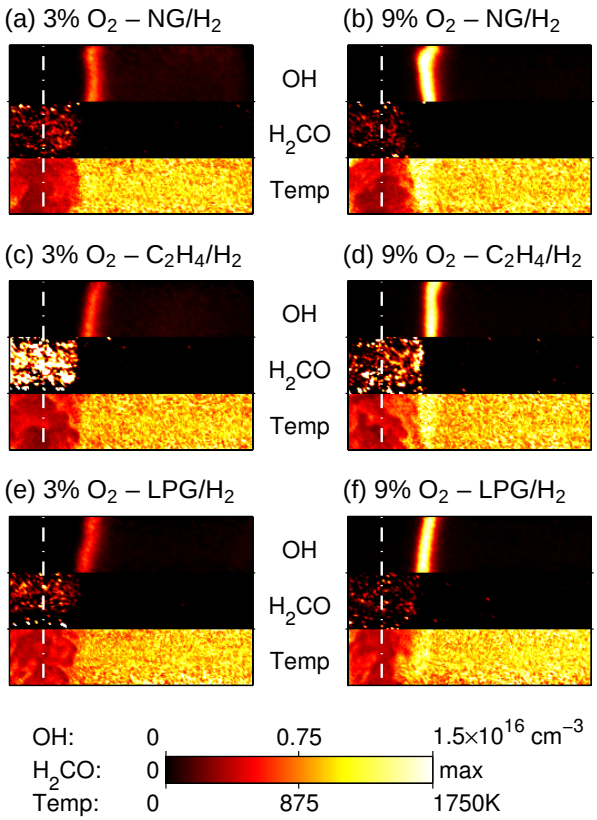

Figure 4: Selection of instantaneous OH, H_2CO and temperature image triplets of natural gas/H_2, C_2H_4/H_2 and LPG/H_2 flames showing typical features. OH shown in number density (molecules/cm^3), H_2CO in arbitrary units, temperature in Kelvin. Re_{jet}=10,000. Each image 8×35mm. Jet centreline marked with dashed line. Axial location 35mm above jet exit.

very low, almost indistinguishable temperature rise across the reaction zone has been seen in a similar high temperature oxidant stream environment [5] and also in a MILD combustion furnace [10]. The low measured temperatures are believed to be genuine, and not because of interferences or problems with the Rayleigh to temperature conversion process. Noteworthy is that the laser-based measurements of the jet and coflow temperatures agree well with those expected, and were also confirmed with a thermocouple.

The H_2CO concentration varies with both the O_2 level and even more dramatically with the type of fuel. Most notably, the 3% O_2 C_2H_4/H_2 flame has significantly higher H_2CO than any other flame. In all cases the H_2CO appears quite uniformly distributed and always exists on the fuel-rich side of the OH layer. The broad radial distribution of H_2CO is also seen in strained laminar flame calculations [7].

Reaction Zone Weakening

The majority of images in the data set appear similar to those in Figure 4, in that they do not show evidence of large-scale turbulent structures. Nevertheless, a proportion of the images do in fact appear convoluted, as determined by curvature of the OH layer, which indicates interaction of the reaction zone with large-scale vortices. Examples of the interaction of the flame front and large-scale vortices are shown in Figure 5. The size of the vortical structures in these images is approximately the integral length scale (∼5mm).

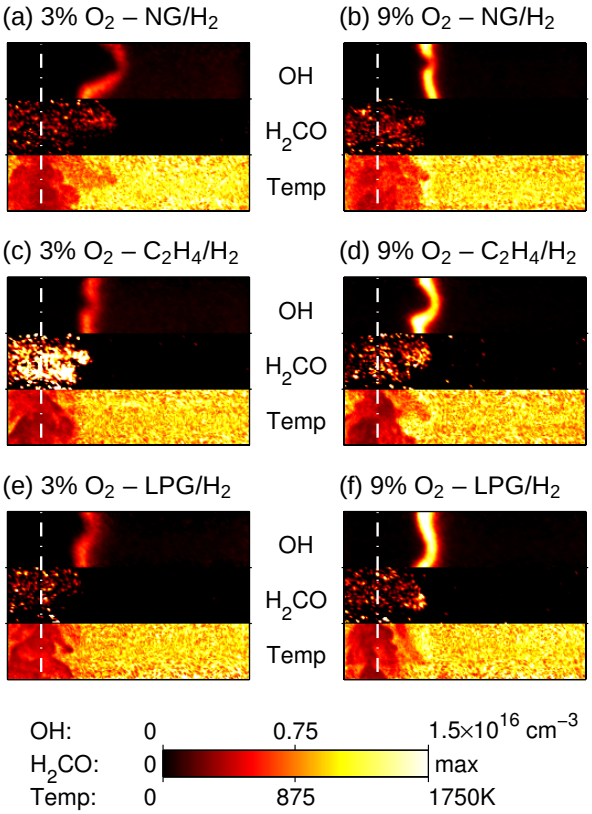

Figure 5: Selection of instantaneous OH, H_2CO and temperature image triplets of natural gas/H_2, C_2H_4/H_2 and LPG/H_2 flames showing vortex interaction with the reaction zone (reaction zone weakening). OH shown in number density (molecules/cm^3), H_2CO in arbitrary units, temperature in Kelvin. Re_{jet}=10,000. Each image 8×35mm. Jet centreline marked with dashed line. Axial location 35mm above jet exit.

As the flame front becomes convoluted and stretched by vortices, the OH images can show a localised decrease in concentration and a spatial thinning of the OH layer. The decrease in OH levels is defined as a weakening of the reaction zone. It is important to recognise that despite a weakening (i.e. a reduction in OH) an actual rupture of the OH layer is never observed. Accompanying the weakening of the flame front can be an increase in H_2CO levels. An increase of H_2CO with strain has previously been noted [8].

Examples of weakening of the reaction zone (and subsequent increases in the H_2CO levels) are noted in both the 3% & 9% O_2 levels. In such cases it is apparent that the flow structure has an effect on the reaction zone. It is apparent that all of the fuels are susceptible to this phenomenon. For the LPG/H_2 flames, the effects are not quite as apparent. Nevertheless the same processes occur, albeit on a more subtle level.

Radial Profiles

The instantaneous images presented (Figures 4 & 5) suggest that each of the various fuel types have a very similar structure. This is also seen in the radial plots of Figure 6. At the 3% O_2 coflow the mean OH profiles seem quite coincident, with each fuel having a similar peak mean value and similar spatial shape. In both the mean and RMS, there is a slight shift of the OH profiles inward towards the centreline as the fuel complexity is increased. This radial shift corresponds to a drop in jet velocity required to maintain the jet Reynolds number. At the 9% O_2 coflow the radial shift of the OH peak with the fuel type is more noticeable. Also more noticeable for the 9% case is a variation in the mean OH peak, although the changes are still relatively small. Worth noting is that despite an almost three-fold difference in the jet exit velocity for the various fuels, because the Reynolds number is constant in all cases, the OH RMS is comparable for either O_2 level.

At both coflow O_2 levels, in the H_2CO profiles of Figure 6 a very significant increase is noted for the C_2H_4/H_2 flame. The mean H_2CO is distributed widely across the radial profiles, but does show evidence of a dip along the jet centreline. The broad radial distribution of H_2CO has already been noted in the instantaneous images, and is consistent with strained laminar flame calculations. The H_2CO levels in the C_2H_4/H_2 flame are significantly higher with the 3% O_2 coflow as compared to 9% O_2, but for the other fuels (natural gas/H_2 & LPG/H_2) the H_2CO is similar at either O_2 level.

As was noted in the instantaneous images, the temperature rise across the reaction zone in the 3% O_2 coflow is barely discernable. For the 3% O_2 LPG/H_2 flame the temperature rise is not resolved in the mean profile. The lack of temperature rise has already been discussed in the typical instantaneous images. At the 9% O_2 coflow, again the LPG/H_2 flame shows the lowest reaction zone temperature. The trends relating to the location of the peak temperature follows the same trend as seen in the OH profiles, viz. the peak shifts towards the centreline as the fuel complexity increases.

Discussion

From the instantaneous images and the radial profiles that have been presented there does not seem to be any significant effect of the fuel type on the structure of the reaction zone. The trends obtained from methane and propane fuels have previously been noted as being similar in a heated and diluted oxidant stream in a spectral emission study [6].

Of the measured scalars, the H_2CO number density changes the most between the different fuel types considered. Nonetheless, the basic behaviour of the H_2CO is essentially constant between the different fuel cases. Changes in the flow structure are also apparent for the different fuel types. These differences arise because of the different jet velocity for each fuel type (required to maintain constant Reynolds number). Despite these minor differences, the fuel type does not lead to any major changes in the overall flame characteristics at the measurement locations.

The photographs of the flames (Figure 3) provide supplemental evidence supporting the similarity of the different fuel types when in the confines of the hot and diluted coflow. Further downstream, after the effects of the coflow have diminished, each of the flames visually appear significantly different. This is suggestive of the importance of the coflow in establishment of the unique conditions which lead to the similarity between the different fuels.

Table 1 shows the average of the peak OH values in each of the images for a particular flame. Also included is the standard deviation (as a percentage) of the values. In determining the peak value in each of the images, only the central 3mm portion of the image is included to avoid over-corrected values towards the edges of the images where the low laser power makes sheet corrections less reliable. Table 1 reiterates the similarity of the OH levels for the different fuel compositions. At either O_2 level the mean peak OH number density is very similar for each fuel. Consistent with the radial profiles, the similarity is especially noted for the 3% O_2 case.

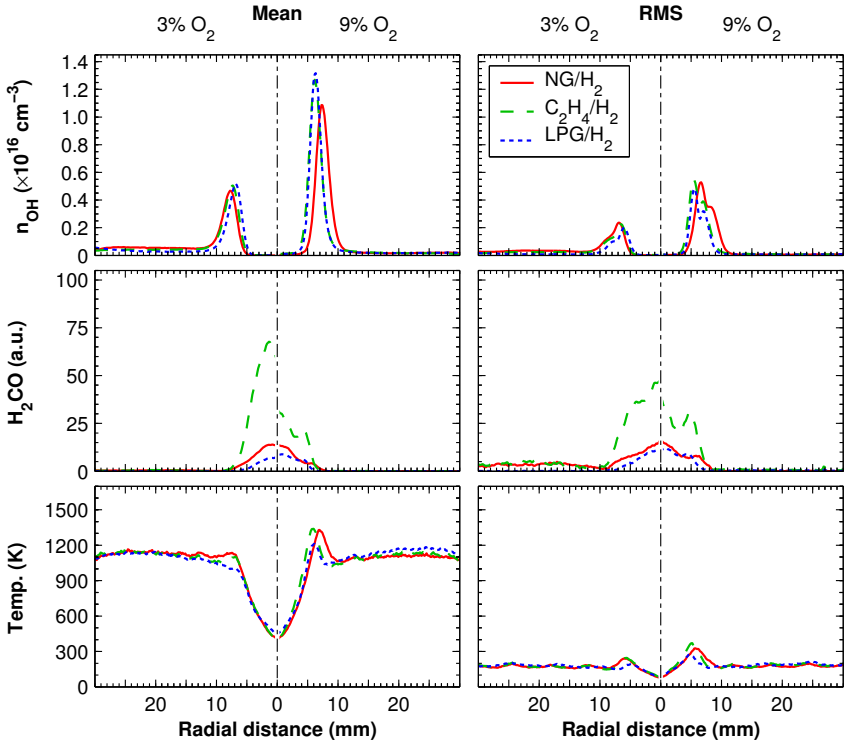

Figure 6: Mean and RMS radial profiles of OH, H_2CO and temperature for natural gas/H_2, C_2H_4/H_2 and LPG/H_2 flames. OH shown in number density (molecules/cm^3), H_2CO in arbitrary units, temperature in Kelvin. Re_{jet}=10,000. Central 3mm strip of images used. Axial location 35mm above jet exit.

Fuel composition	Peak n_{OH} [σ] ($\times 10^{16}$cm^{-3}) 3% O_2	9% O_2
NG/H_2	0.56 [11%]	1.28 [11%]
C_2H_4/H_2	0.56 [10%]	1.53 [30%]
LPG /H_2	0.54 [9%]	1.33 [8%]

Table 1: Mean and standard deviation (σ, in brackets) of peak OH number density measurements. Central 3mm strip of images used. Axial location 35mm above jet exit.

Fuel composition	Peak temp. (K) 3%	9%	Peak n_{OH} (10^{16}cm^{-3}) 3%	9%	Peak n_{H_2CO} (10^{14}cm^{-3}) 3%	9%
CH_4/H_2	1400	1876	0.40	2.04	1.15	1.93
C_2H_4/H_2	1403	1856	0.46	2.11	2.59	0.87
C_3H_8/H_2	1384	1807	0.43	1.97	1.60	1.45

Table 2: Peak temperature and OH & H_2CO number density (molecules/cm^3) from strained laminar flame calculations for 3% and 9% O_2 oxidant stream conditions (a≈200s^{-1}).

At the 35mm location, where the oxidant composition is well defined and not yet affected by surrounding air entrainment, comparisons of the trends can be made to strained laminar flame calculations. Table 2 presents the peak temperature, and the maximum number density of OH and H_2CO for each fuel type and at both O_2 levels obtained from OPPDIF calculations of the Chemkin package using GRI-Mech 3.0 mechanism.

Comparing Tables 1 & 2 it is seen that calculations support the measurements, in that the OH concentration does not change significantly with the fuel composition. The experimental peak OH value for the 3% O_2 flames is higher than from the calculations, whereas at 9% O_2 the calculated value is higher than that found from the experiment. The typical differences between the measured value and calculations is approximately 25% for 3% O_2 and ∼40% for 9% O_2. Nevertheless, there is good similarity of the trends, and also a similar order of magnitude between the experiments and calculations.

Table 2 shows that the H_2CO in the C_2H_4/H_2 flame behaves the opposite to the other two fuels. For C_2H_4/H_2 the H_2CO significantly increases at the lower O_2 case. In contrast, the effect of O_2 on H_2CO is comparatively minor for the other fuels. For C_3H_8/H_2 there is little difference between the two O_2 levels. In the CH_4/H_2 flame the trend is reversed and H_2CO slightly increases with O_2 level. The different behaviour of the H_2CO in the C_2H_4/H_2 flames to the other fuels was also apparent in the experimental data presented. Of particular note in the C_2H_4/H_2 flames was that the H_2CO levels in the 3% O_2 flames was much higher than the other cases, which is consistent with the laminar flame calculations (Table 2). At 9% O_2, Table 2 indicates that the C_2H_4/H_2 flame should have lower H_2CO than the other flames, which is not seen in the experimental data. Nevertheless, in general, the trends of H_2CO largely follow those predicted by the flame calculations shown in Table 2.

It is important to highlight that each of the primary fuels are diluted with hydrogen (H_2) in equal volumetric parts. The addition of H_2 is necessary to increase the flame stability to prevent blowoff. The H_2 added to the fuel stream seems to influence the kinetics such that the different hydrocarbon fuels show similar characteristics.

Conclusions

The comparison between the three different gaseous hydrocarbon fuels in this paper reveal that the fuel type does not have a significant effect on the reaction zone structure under MILD combustion conditions. The fuels considered were natural gas, ethylene, and LPG (each diluted with hydrogen 1:1 by volume). Both from measurements and strained laminar flame calculations the OH concentrations results were seen to be quite constant. Only minor changes of the OH spatial distribution were noted, and attributable to differences in fuel velocity required to maintain constant Reynolds number. The only significant changes with the fuel type were noted in the H_2CO levels, most notably with the C_2H_4/H_2 flame. The trends in the measured H_2CO levels were seen to be consistent with flame calculations.

The similarity of the combustion characteristics for the various gaseous hydrocarbon fuels considered suggests that MILD combustion should be readily adapted for different fuel types. The insensitivity to fuel type is potentially a significant advantage for the implementation and application of MILD combustion to practical systems.

Acknowledgments

The authors would like to thank Dr Zeyad Alwahabi for his assistance with this project. The financial support of The University of Adelaide and the Australian Research Council is gratefully acknowledged.

References

[1] Ahn, C., Akamatsu, F., Katsuki, M. & Kitajima,A., *Fourth Asia-Pacific Conference on Combustion*, 2003, 40–43.

[2] Cavaliere, A. & de Joannon, M., Mild combustion, *Prog. Energy Combust. Sci.*, **30**, 2004, 329–366.

[3] Dally, B. B., *The 1999 Australian Symposium on Combustion & Sixth Australian Flame Days*, Newcastle, Australia.

[4] Dally, B. B., Karpetis, A. N. & Barlow, R. S., *Proc. Combust. Inst. 29*, 2002, 1147–1154.

[5] Gordon, R. L., Dunn, M. J., Masri, A. R. & Bilger, R. W., *Fourth Australian Conference on Laser Diagnostics in Fluid Mechanics and Combustion*, The University of Adelaide, South Australia, Australia, 2005, 45–48.

[6] Ishiguro, T., Tsuge, S., Furuhata, T., Kitagawa, K., Arai, N., Hasegawa, T., Tanaka, R. & Gupta, A. K., *Proc. Combust. Inst. 27*, 1998, 3205–3213.

[7] Medwell, P. R., Kalt, P. A. M. & Dally, B. B., *Combust. Flame*, 2007, doi:10.1016/j.combustflame.2007.09.003.

[8] Medwell, P. R., Kalt, P. A. M. & Dally, B. B., *Combust. Flame*, **148**, 2007, 48–61.

[9] Najm, H. N., Paul, P. H., Mueller, C. J. & Wyckoff, P. S., *Combust. Flame*, **113**, 1998, 312–332.

[10] Özdemir, I. B. & Peters, N., *Exp. Fluids*, **30**, 2001, 683–695.

[11] Plessing, T., Peters, N. & Wünning, J. G., *Proc. Combust. Inst. 27*, 1998, 3197–3204.

[12] Wünning, J. A. & Wünning, J. G., *Prog. Energy Combust. Sci.*, **23**, 1997, 81–94.

[13] Wünning, J. G., FLOX® — Flameless Combustion, *Thermprocess Symposium 2003*, WS Wärmeprozesstechnik GmbH, 2003.